Articles

Effect of Initiator and Ligand Structures on ATRP of Styrene and Methyl Methacrylate Initiated by Alkyl Dithiocarbamate

Yungwan Kwak and Krzysztof Matyjaszewski*

Center for Macromolecular Engineering, Department of Chemistry, Carnegie Mellon University, 4400 Fifth Avenue, Pittsburgh, Pennsylvania 15213

Received June 2, 2008; Revised Manuscript Received July 11, 2008

ABSTRACT: Atom transfer radical polymerization (ATRP) of styrene (St) and methyl methacrylate (MMA) initiated by various alkyl diethyldithiocarbamate (DC) initiators was successfully carried out in the presence of copper catalysts with nitrogen-based ligands. Well-controlled polymerizations with narrow molecular weight distribution (M_w/M_n < 1.1 (St) and M_w/M_n < 1.2 (MMA)) were achieved in both polymerizations. The polymerization rate followed first-order kinetics with respect to monomer conversion, and the molecular weight of the polymers increased linearly up to high conversion. Initiation efficiency of both polymerizations was strongly dependent on the structure of a DC. The results of ^{1}H NMR analysis of low-mass model compounds and chain extension confirmed that well-defined polystyrene bearing a DC group as the active chain end was obtained via ATRP of St with a DC initiator. Ligand structure and ligand/copper ratio also strongly affected the degree of control attained in the polymerization. Activation rate constants and equilibrium constants of ATRP with DC initiators and copper complexes were determined. The results of cyclic voltammetry with the $Cu^{II}DC_2$ complex indicated that it has more negative reduction potential and, consequently, higher (pseudo)halidophilicity than those of $Cu^{II}Br_2$ or $Cu^{II}Cl_2$ with the same ligand Me_6TREN.

Introduction

Controlled/living radical polymerization (CRP) became one of the robust and powerful techniques for polymer synthesis[1−4] during the past decade. CRP can be achieved by maintaining a dynamic equilibrium between a dormant species and propagating radicals via a reversible deactivation procedure.[5] Several techniques have been developed to attain this equilibrium, including stable free-radical polymerization,[6,7] atom transfer radical polymerization (ATRP),[8−13] reversible addition−fragmentation chain transfer polymerization,[14−16] Te-, Sb-, and Bi-mediated polymerization,[17−20] and reversible chain transfer catalyzed polymerization.[21]

ATRP,[8−13] in particular, is one of the most efficient CRP methods, allowing the synthesis of novel (co)polymers with a predetermined degree of polymerization and narrow molecular weight distribution, the incorporation of a wide range of functional monomers, and the preparation of controllable macromolecular structures under mild reaction conditions. ATRP generally requires an alkyl halide (R−X) or pseudo-halide[22,23] as an initiator and a transition metal complex (Cu,[9] Ru,[10] Os,[24] Mo,[25,26] or Fe,[27,28] for example) as a catalyst. ATRP involves homolytic cleavage of an R−X bond by a transition metal complex, such as Cu^IX/L (with a rate constant k_a), followed by propagation (with a rate constant k_p) and reversible deactivation of the propagating chain radical ($R^•$) (with a rate constant k_{da}) by the higher oxidation state catalyst complex, $Cu^{II}X_2/L$. The reaction progresses by repetitive transfer of halogen or pseudo-halogen atoms to and from the transition metal complex (Scheme 1).[5]

* Corresponding author: Tel +1-412-268-3209; e-mail km3b@andrew.cmu.edu.

Scheme 1. Basic Mechanism for Atom Transfer Radical Polymerization (ATRP)

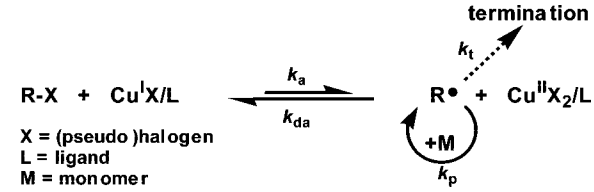

The development of new catalysts and the reduction of the required catalyst concentration are topics of great interest in the improvement of ATRP. For example, the development of two new initiation techniques, known as activators regenerated by electron transfer (ARGET)[29−33] and initiators for continuous activator regeneration (ICAR)[29] ATRP, permitted polymerizations with dramatically lower catalyst concentrations, which do not require removal of the catalyst from the final product.

Recent studies on bond dissociation energy (BDE) of alkyl (pseudo)halides proved that the activity of ATRP initiators depends reciprocally on the alkyl (pseudo)halide BDE.[34,35] Furthermore, a systematic study on the effects of the initiator structure on initiation activity was recently reported.[36] These studies resulted in two general conclusions: (1) The activity of alkyl group in initiators follows the order of 3° > 2° > 1° and phenyl ester > nitrile > ester > benzyl > amide. (2) The activity of the leaving atom (or group) decreases in the order of I ≥ Br > Cl ≫ pseudo-halide.

Iniferter polymerization was one of the earliest CRP techniques reported by Otsu and co-workers in 1982 as a novel method for preparing well-defined polymers.[37−39] It was demonstrated recently that this iniferter technique can also be

10.1021/ma801231r CCC: $40.75
Published on Web 08/20/2008

Scheme 2. Chemical Structures of Alkyl Diethyldithiocarbamate Initiators

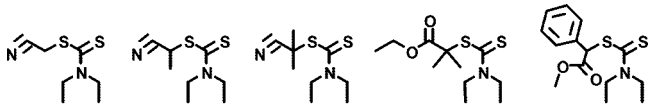

used to prepare complex macromolecular structures[40−43] such as block copolymers, graft copolymers, and star and hyperbranched polymers. However, the structures and compositions of the polymers were relatively poorly controlled with high polydispersity (PDI = M_w/M_n > 2.0). Some improvements in iniferter polymerization were made in the presence of copper catalyst. When the reverse ATRP of methyl methacrylate (MMA) was carried out in the presence of copper(II) *N*,*N*-diethyldithiocarbamate, poly(methyl methacrylate) (PMMA) with relatively narrow molecular weight distribution was obtained, but the initiation efficiency was low and a large amount of radical initiator was used, resulting in a high level of chain termination.[44,45] Also, when normal ATRP of MMA and styrene (St) was initiated by ethyl 2-*N*,*N*-(diethylamino)-dithiocarbamoylbutyrate and (1-naphthyl)-methyl *N*,*N*-diethyldithiocarbamate, low initiation efficiency and relatively low molecular weight PMMA and polystyrene (PSt) were formed.[46−49]

In the current study, we focused on synthesis and systematic kinetic studies of several new iniferter initiators as well as reactivity of various Cu complexes. This study generated a more comprehensive structure−reactivity correlation and provided new guidelines for selection of the efficient catalysts and initiators to generate well-defined low-polydispersity PSt and PMMA. We demonstrated by the low-mass model experiments that no exchange occurred between DC and halogen in the copper catalyst. We also systematically analyzed polymerization kinetic parameters, namely k_a and K_{ATRP} (= k_a/k_{da}), and the effect of initiator and ligand structure on the degree of control attained in the polymerization. Furthermore, redox potential and halidophilicity of this system were studied.

Experimental Section

Synthesis of Iniferter Initiators. Cyanomethyl diethyldithiocarbamate (CMDC), 1-cyanoethyl dithiocarbamate (ANDC), 1-cyano-1-methylethyldiethyldithiocarbamte (MANDC), 2-(*N*,*N*-diethyldithiocarbamyl)isobutyric acid ethyl ester (EMADC), and methyl{[(diethylamino)carbonothioyl]thio}(phenyl)acetate (MPADC) (Scheme 2) were synthesized as follows.

CMDC was prepared according to the previously reported literature procedures.[50] The sodium salt of *N*,*N*-diethyldithiocarbamate, NaDC (8.80 g, 1.2 equiv), was added to a solution of 3.00 g (1.0 equiv) of bromoacetonitrile in 200 mL of acetone, and the reaction mixture was stirred at 40 °C for 16 h. The white precipitate was removed by filtration, and acetone was evaporated from the mixture. The residue was dissolved in benzene, and any insoluble solid was again removed by filtration, after which the benzene was removed by evaporation. The crude oil was distilled under reduced pressure at 103−105 °C (1 mmHg) to obtain a light yellow viscous liquid. Purity (>98%) was determined by ^{1}H NMR. ^{1}H NMR ($CDCl_3$, δ, ppm): 4.25 (s, 2H), 3.65−4.15 (m, 4H), 1.25−1.45 (s, 6H).

ANDC. 5 g of 2-bromopropionitrile and 10.10 g of NaDC were used in a procedure similar to that described above providing a crude oil which was distilled at 105−110 °C (1 mmHg); purity was ca. 97%. ^{1}H NMR ($CDCl_3$, δ, ppm): 4.95−5.05 (q, 1H), 3.64−4.08 (m, 4H), 1.71−1.75 (d, 1H), 1.24−1.37 (s, 6H).

EMADC. 5 g (1.0 equiv) of ethyl 2-bromoisobutyrate and 6.94 g (1.2 equiv) of NaDC were also used in a similar procedure, providing a crude oil which was distilled at 115−125 °C (1 mmHg) to give a light yellow viscous liquid; purity was ca. 98%. ^{1}H NMR ($CDCl_3$, δ, ppm): 4.15−4.28 (q, 2H), 3.62−4.06 (m, 4H), 1.71−1.78 (s, 6H), 1.19−1.37 (s, 9H).

MANDC. [51] Tetraethylthiuram disulfide (9.03 g, 1.0 equiv) was added to a solution of 7.5 g (1.5 equiv) of AIBN in 100 mL of toluene, and the reaction mixture was bubbled with nitrogen for 30 min and then stirred at 55 °C for 65 h. The white precipitate was removed by filtration, and toluene was removed by evaporation from the mixture. The crude oil was distillated under reduced pressure, 107−115 °C 1 mmHg, providing a light yellow viscous liquid; purity was ca. 97%. ^{1}H NMR ($CDCl_3$, δ, ppm): 3.61−4.11 (m, 4H), 1.89−1.98 (s, 6H), 1.22−1.39 (s, 6H).

MPADC. NaDC (3.25 g, 1.1 equiv) was added to a solution of 3.00 g (1.0 equiv) of methyl α-bromophenylacetate in 100 mL of acetone, and the reaction mixture was stirred at rt for 5 h. The white precipitate was removed by filtration, and acetone was evaporated from the mixture. The crude mixture was dissolved in benzene, and any insoluble solid was removed by filtration, after which the mixture was kept at −10 °C overnight and the white needle-like precipitation was again removed by filtration. The filtrate was evaporated to dryness; purity was ca. 98%. ^{1}H NMR ($CDCl_3$, δ, ppm): 7.29−7.51 (m, 5H), 5.84 (s, 1H), 3.62−4.09 (m, 4H), 3.38 (s, 3H), 1.25−1.39 (s, 6H).

Monomers and Other Reagents. St and MMA (Aldrich, 99%) were passed through a column filled with basic alumina, dried over calcium hydride, and distilled under reduced pressure. *N*,*N*-Bis(2-pyridylmethyl)octadecylamine (BPMODA), 4,4′,4″-tris(5-nonyl)-2,2′:6′,2″-terpyridine (tNtpy), tris(2-(dimethylamino)ethyl)amine (Me_6TREN), and tris-[(2-pyridyl)methyl]amine (TPMA) were synthesized according to procedures previously reported in the literature.[52] Cu^IDC was prepared according to previously reported literature procedures.[53] Copper(I) bromide (Aldrich, 99.999%), tetraethylthiuram disulfide (Aldrich, 97%), NaDC (Aldrich, 99%), 2,2,6,6-tetramethylpiperidinyl-1-oxy (TEMPO, Aldrich, 99%), 2,2′-bipyridine (bpy, Aldrich, 99%), *N*,*N*,*N*′,*N*′-tetramethylethylenediamine (TMEDA, Aldrich, 99%), PMDETA (Aldrich, 99%), and *N*,*N*,*N*′,*N*″,*N*‴,*N*‴-hexamethyltriethylenetetramine (HMTETA, Aldrich, 97%) were used as received. All the other reagents and solvents were used as received.

Analyses. The number- and weight-average molecular weight M_n and M_w, respectively, and polydispersity were determined by gel permeation chromatography (GPC). The GPC was conducted with a Waters 515 pump and a Waters 410 differential refractometer using PSS columns (Styrogel 10^5, 10^3, 10^2 Å) in tetrahydrofuran (THF) as an eluent at 30 °C at a flow rate of 1 mL/min. The column system was calibrated with standard linear PSts and PMMAs. Conversion of all monomers was determined with known concentrations of polymers in THF. ^{1}H NMR spectra were recorded using a Bruker 300 MHz spectrometer with a delay time of 1 s. Deuterated acetonitrile (MeCN-d_3) was used as the solvent for model reaction, and $CDCl_3$ was used for initiator and polymer chain-end analysis. A Cary 5000 UV/vis/NIR spectrometer (Varian) was used for determining Cu^{II} concentration. A Gamry Reference 600 potentiostat was used for determining redox potential of Cu^{II} complex.

General Polymerization Procedures. In a typical experiment, CuBr (41.3 mg, 0.29 mmol) was added to a dried Schlenk flask equipped with a stir bar. After sealing with a rubber septum, the flask was degassed and backfilled with nitrogen (N_2) five times and then left under N_2. Subsequently, a mixture of St (3.00 g, 28.9 mmol), initiator, and ligand was added to a glass vial and degassed by three freeze−pump−thaw cycles. It was then transferred to the Schlenk flask, which was placed in a thermostated oil bath at the desired temperature. Samples were taken periodically under N_2 using an N_2-purged syringe, diluted by THF to a known concentration, passed through a column filled with neutral alumina to remove the copper complex, and analyzed by GPC.

Typical Procedure for Measurement of Activation Rate Constant (k_a) and Equilibrium Constant (K_{ATRP}) (CuBr/PMDETA with EMADC). The experimental procedure used to determine the values of k_a and K_{ATRP} by UV is similar to that provided in previous publications detailing the determination of k_a

or K_{ATRP}.[52,54] To measure k_a, CuBr/PMDETA (10.0 mM), TEMPO (10.0 mM, without TEMPO in the case of K_{ATRP} measurement), and MeCN were mixed in a Schlenk flask joined to a quartz UV cuvette, and the flask was transferred to a Cary 5000 UV/vis/NIR spectrometer (Varian). The degassed EMADC (1.0 mM) was injected via a N_2-purged syringe. The absorbance at a wavelength corresponding to the λ_{max} of the generated Cu^{II} deactivator complex was monitored at timed intervals. The concentration of the deactivator generated in the system was calculated using values of the extinction coefficients for the Cu^{II} complexes determined separately.[55] Other combinations of initiators and Cu^{I} complexes were studied in a similar fashion.

End-Group Analysis by Model Reaction. CuBr (50 mM) was added to a dried Schlenk flask equipped with a stir bar. After sealing with a rubber septum, the flask was degassed and backfilled with N_2 five times and then left under N_2. Subsequently, the mixture of PMDETA (50 mM) in MeCN-d_3 was added to a glass vial and degassed by three freeze−pump−thaw cycles. The solution was then transferred to the Schlenk flask and stirred until all CuBr dissolved. Degassed MANDC (50 mM) was injected and the flask was shaken. The mixture was transferred to an NMR tube end-sealed with a rubber septum, and the NMR spectrum was measured. End-group analysis with Cu^{I}DC was carried out by a method similar to the one described above.

Macroinitiator Synthesis. CuBr (275 mg) was added to a dried Schlenk flask equipped with a stir bar. After sealing with a rubber septum, the flask was degassed and backfilled with N_2 five times and then left under N_2. Subsequently, St (10.0 g), PMDETA (998 mg), and EMADC (253 mg) were added to a glass vial and degassed by three freeze−pump−thaw cycles. The solution was then transferred to the Schlenk flask, which was placed in a thermostated oil bath at 120 °C. The polymerization was stopped after a 45 min reaction by opening the flask and exposing the catalyst to air. The mixture was diluted with 20 mL of dichloromethane and passed through a neutral alumina column. The solution was concentrated by rotary evaporation, and the polymer was precipitated by addition to a large amount of cold methanol. Dissolution and precipitation were repeated until a white powder was obtained. The precipitated polymer was dried in a vacuum oven at 40 °C until a constant weight was reached and analyzed by GPC (M_n = 1900, M_w/M_n = 1.06).

Chain Extension of PSt Macroinitiator with St. The PSt macroinitiator (200 mg, 0.11 mmol) and PMDETA were dissolved in St (2.22 g, 21.3 mmol) in a 10 mL round-bottom flask and subjected to a freeze−pump−thaw cycle three times. This solution was transferred to a Schlenk flask containing degassed CuBr (30.5 mg, 0.21 mmol). The flask was then placed in a thermostated oil bath at 120 °C. The polymerization was stopped after 340 min (M_n = 20 600, M_w/M_n =1.08) by opening the flask and exposing the catalyst to air.

Cyclic Voltammetry. All voltammograms were measured at 25 °C with a Gamry Reference 600 potentiostat. Solutions of Cu^{II} complex (1.0 mM) were prepared in a dry solvent containing 0.1 M NBu_4PF_6 as the supporting electrolyte. Measurements were carried out under N_2 at a scanning rate of 0.1 V s^{-1} using a glassy carbon disk as the working electrode and a platinum wire as the counter electrode. Potentials were measured vs SEC using a 0.1 M NBu_4PF_6 salt bridge to minimize contamination of the analyte with Cl^- ions.

Results and Discussion

ATRP of St. Before conducting ATRP in the presence of a DC initiator and copper catalyst, a thermal iniferter polymerization of St was performed, as a reference example. The polymerization was carried out at 120 °C with the ratio of St/EMADC = 100/1. It can clearly be observed in Figure 1 that the number-average molecular weight (M_n) does not increase linearly with conversion when EMADC is used as a thermal initiator but actually decreases as a function of conversion. This behavior is in accordance with known RAFT procedures, in which EMADC is an inefficient control agent (i.e., the chain transfer constant (C_{tr}) is close to or smaller than unity).[56] This is in agreement with low C_{tr} of polystyrene radicals with iniferters, namely, tetramethylthiuram disulfide or 1-(*N*,*N*-diethyldithiocarbamyl)ethylbenzene (C_{tr} = 0.29 and 4.4 × 10^{-3} at 60 °C, respectively).[50]

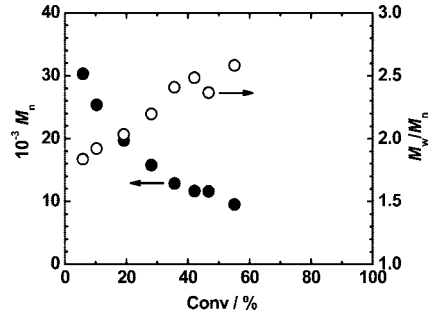

Figure 1. Dependence of number-average molecular weight, M_n (●), and polydispersity, M_w/M_n (○), vs conversion for the bulk polymerization of styrene at 120 °C: St/EMADC = 100/1. Note that molecular weight decreases and polydispersity increases with conversion.

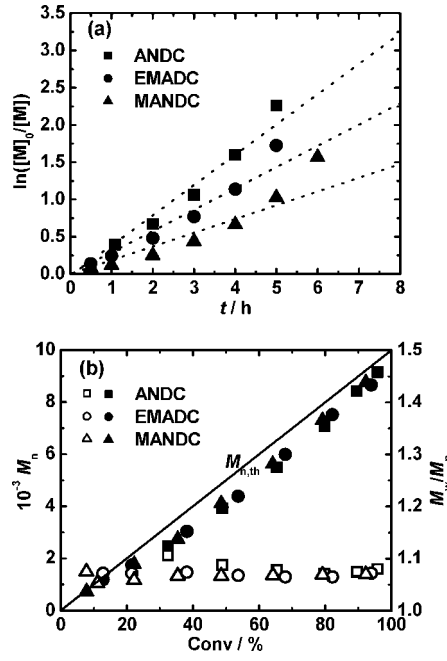

Figure 2. (a) Kinetic plot in the bulk polymerization of styrene at 120 °C with PMDETA ligand and (b) dependence of number-average molecular weight, M_n (■, ●, and ▲) M_w/M_n (□, ○, and △), vs conversion for the bulk polymerization of styrene at 120 °C: St/DC initiator/CuBr/PMDETA = 100/1/1/1.

In the following studies, ATRP of St was carried out using various DC initiators, namely, CMDC, ANDC, MANDC, EMADC, and MPADC. The polymerization was conducted at 120 °C with a ratio of St/DC initiator/CuBr/PMDETA = 100/1/1/1. Figure 2a shows the linear kinetic plot of monomer conversion, suggesting that a constant radical concentration is maintained. Figure 2b shows the evolution of M_n and M_w/M_n with conversion. All polymerizations using ANDC, EMADC, and MANDC as initiators appeared to be well controlled; the molecular weights (MW) of PSt increased linearly with conversion, agreeing well with the theoretical values ($M_{n,th}$), and low M_w/M_n (<1.10) were observed. If one compares Figure 1 and 2, it can be clearly seen that polymerizations conducted in the presence of the copper complex brought significant improvement in control over the polymerization, in terms of both MW and PDI. However, the ATRP of St using CMDC resulted only in

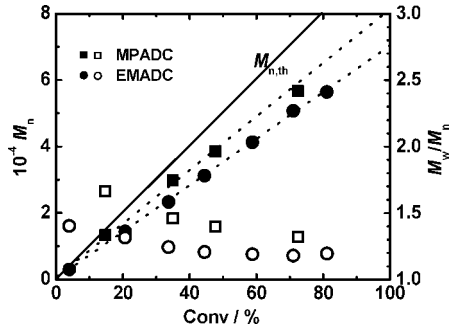

Figure 3. Dependence of number-average molecular weight, M_n (■ and ●), and polydispersity, M_w/M_n (□ and ○), vs conversion for the bulk polymerization of styrene at 120 °C: St/EMADC (or MPADC)/CuBr/PMDETA = 1000/1/2/2.

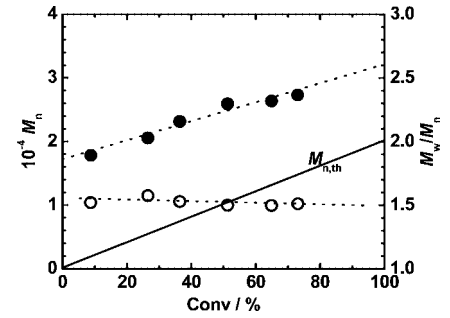

Figure 4. Dependence of number-average molecular weight, M_n (●), and polydispersity, M_w/M_n (○), vs conversion for the bulk polymerization of MMA at 100 °C with EMADC initiator: MMA/EMADC/CuBr/bpy = 200/1/1/2.

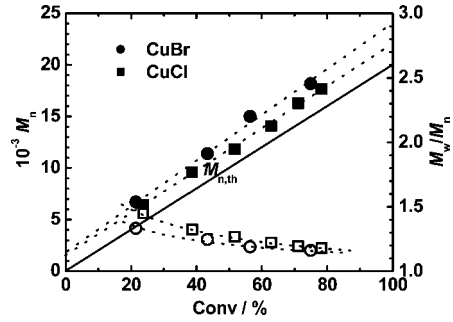

Figure 5. Dependence of number-average molecular weight, M_n (● and ■), and polydispersity, M_w/M_n (○ and □), vs conversion for the bulk polymerization of MMA at 100 °C with MANDC initiator: MMA/MANDC/CuBr (or CuCl)/bpy = 100/1/1/2.

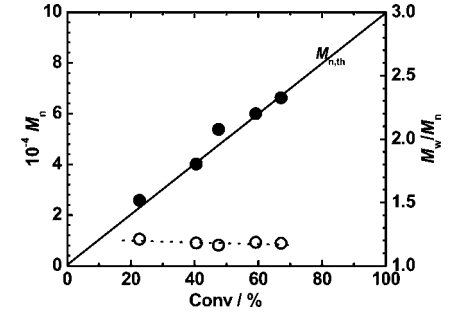

Figure 6. Dependence of number-average molecular weight, M_n (● and ■), and polydispersity, M_w/M_n (○ and □), vs conversion for the bulk polymerization of MMA at 100 °C: MMA/MANDC/CuBr/bpy = 1000/1/1/2.

low conversion (ca. 7%) at 120 °C for 7 h reaction, low MW (M_n < 2000), and a bimodal shape in the GPC chromatogram, whereas the initiator bromoacetonitrile, which is an analogue for CMDC, was used for successful normal ATRP of St.[57] This result indicates that a secondary alkyl group adjacent to the sulfur atom in the initiator is necessary for controlling St polymerization, meaning activity of the substitution group for the initiators increased in the order of primary < second and tertiary.

Higher MW PSt was prepared at 120 °C with a ratio of St/EMADC (or MPADC)/CuBr/PMDETA = 1000/1/2/2 (Figure 3). In both polymerizations, the MW increased linearly with conversion; both MWs showed some deviations from the theoretical value, presumably due to thermal self-initiation process. Final MW reached M_n = 60 000 in both cases at ca. 80% conversion. M_w/M_n was slightly higher at lower conversion, but it reached 1.2−1.3 at higher conversion. These results indicate that well-controlled PSt with MW up to 60 000 was prepared using either MPADC or EMADC as an initiator.

ATRP of MMA. According to previous reports, ATRP of MMA using DC initiators was not successful, in terms of MW and PDI control, due to low initiation efficiency of the DC initiator.[44,45,48] As a reference, polymerization of MMA was carried out at 100 °C with a ratio of MMA/EMADC/CuBr/bpy = 200/1/1/2. The result is shown in Figure 4, and it can be observed that M_n increases with conversion but has a significantly higher value than the theoretical value calculated based on the quantitative initiation. Furthermore, M_w/M_n remained fairly high (ca. 1.5) throughout the polymerization. This behavior is in accordance with previously reported results[44,45,48] and can be related to either inefficient initiation or slow deactivation.[58] A slow deactivation in ATRP can be overcome by the addition of an oxidized form of the catalyst, such as $CuBr_2$.[59] However, no improvement was observed after addition of a small amount of $CuBr_2$ to this polymerization.

Subsequently, MMA polymerization was carried out at 100 °C in the presence of MANDC instead of EMADC with the ratio of MMA/MANDC/CuBr/bpy (or CuCl/bpy) = 200/1/1/2. The result is shown in Figure 5 and indicates a well-controlled polymerization of MMA. The MW of PMMA increased linearly with conversion, agreeing well with theoretical values, and low M_w/M_n (ca. 1.20) were observed. The MW of PMMA with CuCl was slightly closer to the theoretical values than with CuBr, while the M_w/M_n increased slightly. Above results indicate that the activity of the substitution group for the initiators increased in the order of ester < nitrile.

For well-controlled polymers, as described above, initiator selection is a crucial factor, and steric effects should be a primary consideration. This is quite different from normal ATRP[4,36] and rather resembles RAFT polymerization.[14−16] Therefore, model studies are required to explain these results, as will be described in the next sections. Generally, in ATRP, polar effects dominate and should be first taken into account for efficient initiator selection, with steric considerations being less important.[4] For example, the initiator bromoacetonitrile, which is an analogue for CMDC, was used for successful normal ATRP of St,[57] while the ATRP with CMDC was unsuccessful, as described above.

Higher MW PMMA was prepared with a MMA/initiator ratio of 1000/1. The MW was almost identical to the theoretical value, increasing up to 70 000, with M_w/M_n as low as 1.2 from an early stage of polymerization (Figure 6). Both initiation efficiency of the polymerization and control improved when a larger ratio of monomer/initiator was used.

Effect of Ligand Structure. Besides initiator, ligand is another important parameter that affects the level of control in a polymerization. To demonstrate this, the polymerizations of St with EMADC and CuBr were carried out in the presence of

Table 1. Result of St Polymerization Using St/EMADC/CuBr/Ligand = 100/1/1/1 in Bulk at 120 °C

ligand	time (min)	conv (%)	$M_{n,GPC}$	$M_{n,th}$	M_w/M_n
TMEDA	240	41	3400	4100	1.47
	570	99	8800	9900	1.33
PMDETA	30	13	1200	1300	1.07
	360	94	8700	9400	1.07
BPMODA	60	15	1000	1500	1.40
	250	86	7900	8600	1.17
tNtpy	30	21	1500	2100	1.99
	260	52	3100	5200	2.20
HMTETA	60	12	1100	1200	1.28
	690	87	7400	8700	1.32
Me_6TREN	105	-	6100		2.14
TPMA	20	14	1200	1400	2.27
	150	61	5900	6100	2.42

Table 2. Result of MMA Polymerization Using MMA/MANDC/CuBr/Ligand = 100/1/1/1 in Bulk at 100 °C

ligand	time (min)	conv (%)	$M_{n,GPC}$	$M_{n,th}$	M_w/M_n
TMEDA	5	21	5500	4200	1.21
	30	66	20400	13200	1.10
bpy	10	21	6700	4200	1.33
	42	75	18200	15000	1.16
PMDETA	10	20	11400	4000	1.65
	38	53	20600	10600	1.43
BPMODA	5	26	7000	5200	1.39
	40	71	20400	14200	1.18
HMTETA	9	34	10900	6800	1.34
	28	66	18300	13200	1.26

Cu catalyst complexes with different nitrogen-based ligands, such as TMEDA, PMDETA, BPMODA, tNtpy, HMTETA, Me_6TREN, and TPMA. Table 1 summarizes the results. Polymerization with the bidentate ligand, TMEDA, indicated a fairly well controlled, producing PSt with $M_n = 8900$ and $M_w/M_n = 1.33$ at full conversion. The best controlled polymerization was obtained with the tridentate ligand, PMDETA, producing PSt with the lowest M_w/M_n. The tridentate ligand with two pyridine rings along with one alkyl chain, BPMODA, also showed a fairly well-controlled polymerization. On the other hand, the polymerization using the tridentate ligand with three pyridine rings, tNtpy, showed poor control, producing a polymer with MW lower than the theoretical values and with a high M_w/M_n (2.20) even at 52% conversion. Surprisingly, both of the bridged tetradentate ligands, Me_6TREN and TPMA, resulted in uncontrolled polymerization, producing a polymer with high M_w/M_n (>2.1). In contrast, the linear tetradentate ligand, HMTETA, yielded a quite well-controlled polymer. This observation is completely opposite from that of halogen, Br or Cl, based ATRP.[52,60,61] The reason for this can be explained by the further kinetic parameters of k_a and k_{da} (see below).

The result of ATRP of MMA with MANDC and CuBr, carried out in the presence of different nitrogen-based ligands, are shown in Table 2. Polymerization with the bidentate ligands TMEDA and bpy resulted in well controlled polymerizations, producing low PDI polymer, although M_ns were slightly higher than the theoretical ones. The poorest control and consequently the highest PDI for PMMA were obtained using the tridentate ligand PMDETA, which is opposite from the result with styrene polymerization. Both tridentate and tetradentate ligand, BPMODA and HMTETA, showed fairly well-controlled polymerization. These results clearly show that correct ligand selection is very important in order to obtain a well-controlled polymer with DC species. PMDETA is the best ligand for St polymerization, followed by BPMODA, HMTETA, and TMEDA, while both Me_6TREN and TPMA are less efficient ligands for St polymerization with DC initiators. On the other hand, for MMA polymerization the best ligands are bpy and TMEDA, followed by HMTETA and BPMODA.

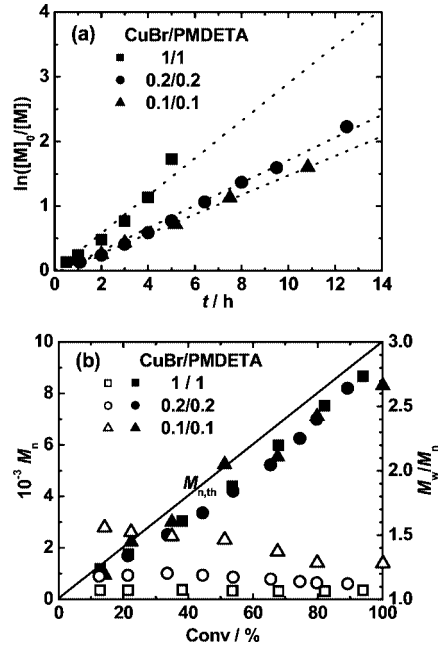

Figure 7. (a) Kinetic plot of the bulk polymerization of styrene at 120 °C with PMDETA ligand and (b) dependence of number-average molecular weight, M_n (■, ●, and ▲), M_w/M_n (□, ○, and △), vs conversion for the bulk polymerization of styrene at 120 °C: St/EMADC/CuBr/PMDETA = 100/1/0.1−1/0.1−1.

Table 3. Result after 4 h Polymerization of St Using St/EMADC/CuBr/PMDETA = 100/1/1/0−3 at 120 °C

entry	$[PMDETA]_0/[CuBr]_0$	$M_{n,GPC}$	$M_{n,th}$	M_w/M_n	conv (%)
1	0	3000	2400	2.00	24
2	0.25	7500	8200	1.14	82
3	0.50	8600	9200	1.10	92
4	0.75	6600	7500	1.08	75
5	1.00	6000	6800	1.07	68
6	2.00	4600	5500	1.09	55
7	3.00	4200	5000	1.09	50

ATRP of St with a Reduced Amount of Catalyst. Figure 7a compares the kinetic results of ATRPs of St at 120 °C using EMADC as initiator at 10, 20, and 100 mol % of catalyst relative to initiator. The plots of $\ln([M]_0/[M])$ are linear. Obviously, ATRP with 100 mol % catalyst is faster than the reaction with 20 mol %, which is slightly faster than that with 10 mol % because the activation reaction is faster with an increased amount of catalyst, resulting in higher radical concentration and thereby a faster polymerization rate. The MW of the resulting PSt increases linearly with conversion and M_w/M_n is low for both 20 and 100 mol % catalyst ratios (Figure 7b). The M_w/M_n of the reaction with 10 mol % catalyst was higher than 1.5 at low conversion, but it finally reached 1.3 at full conversion. All MWs are quite close to the theoretical values, which shows that the initiation efficiency in these polymerizations is basically identical. The above result indicates that one can conduct controlled polymerizations with reduced amounts of copper catalyst and that one needs at least a 10 mol % catalyst relative to initiator to control the polymerization.

Effect of Ligand/Copper Ratio. The ligand/copper ratio is an important parameter in ATRP because it has a strong effect on the polymerization rate and the level of control achieved in the polymerization.[62−67] A series of St polymerizations were carried out while varying the amount of ligand without changing any other parameters. Table 3 summarizes the results after 4 h polymerization. In the absence of any ligand (entry 1), the conversion was only 24% and M_w/M_n was 2.00. In the presence of ligand, the M_w/M_n was quite low and was the lowest when

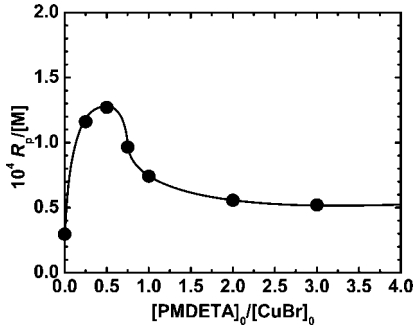

Figure 8. Plot of R_p/[M] vs $[PMDETA]_0/[CuBr]_0$ ratio for the bulk polymerization of St at 120 °C: St/EMADC/CuBr/PMDETA = 100/1/1/0−3 at 120 °C.

Table 4. Activation Rate Constant (k_a), Equilibrium Constant ($K_{ATRP} = k_a/k_{da}$), and Deactivation Rate Constant (k_{da}) with CuBr/Ligand

entry	initiator	ligand	k_a[a] (M^{-1} s^{-1})	K_{ATRP}[b]	k_{da} (M^{-1} s^{-1})	reference
1	EMADC	PMDETA	0.12	2.0×10^{-9}	6.1×10^7	this work
2	EBiB	PMDETA	2.7	7.5×10^{-8}	3.6×10^7	52 and 54
3	MANDC	PMDETA	1.1	8.8×10^{-8}	1.3×10^7	this work
4	EMADC	HMTETA	0.0075			this work
5	EBiB	HMTETA	0.14	1.1×10^{-8}	1.3×10^7	52 and 54
6	MANDC	HMTETA	0.016	2.7×10^{-9}	5.9×10^6	this work
7	EMADC	Me_6TREN	0.0077			this work
8[c]	EBiB	PMDETA	0.87			this work

[a] Values of k_a were measured using $[TEMPO]_0/[ligand]_0/[CuBr]_0/[initiator]_0$ = 10/10/10/1 mM, and only entry 4 was measured using $[TEMPO]_0/[ligand]_0/[CuBr]_0/[initiator]_0$ = 50/50/50/5 mM at rt in MeCN. [b] Values of K_{ATRP} was measured using $[ligand]_0/[CuBr]_0/[initiator]_0$ = 10/10/10 mM (entries 1 and 3) and $[ligand]_0/[CuBr]_0/[initiator]_0$ = 100/100/100 mM (entry 6) at rt in MeCN. [c] Value of k_a was measured using $[TEMPO]_0/[ligand]_0/[Cu^IDC]_0/[EBiB]_0$ = 10/10/10/1 mM at rt in MeCN.

∼ 1/1 ratio of ligand/copper was used (entry 5).

A nearly first-order plot with respect to monomer was observed in the bulk ATRP of St. On the basis of the slope, the calculated values of the rate of polymerization (R_p) as a function of the $[PMDETA]_0/[CuBr]_0$ ratio are shown in Figure 8. A strong dependence between the R_p and the ratio of ligand/copper in the catalyst complex was noticed. Increasing the amount of ligand increased R_p which reached a maximum at $[PMDETA]_0/[CuBr]_0$ ratio = 0.5/1.0. But R_p decreased with further increases in the amount of ligand added to the polymerization. These observations are different from normal ATRP, in which the maximum R_p and best control were obtained at $[PMDETA]_0/[CuBr]_0$ ratio = 1/1. The observed maximum R_p at $[PMDETA]_0/[CuBr]_0$ ratio = 0.5 could be due to the formation of an optimal ratio of activator to deactivator concentration under this condition. In the presence of excess ligand ($[PMDETA]_0/[CuBr]_0$ ratio >1), there is a possibility of degradative chain transfer to the ligand which would decrease the R_p due to the loss of active chains from the reaction.[68]

***K_{ATRP}* and *k_a*.** These results, quite different from normal ATRP, encouraged us to investigate model kinetic studies in order to have a deeper mechanistic insight. The kinetic parameters, k_a and k_{da} (i.e., the activation and deactivation rate constants), are crucial factor for controlling ATRP. K_{ATRP} and k_a of some selected initiator/ligand systems were measured using the modified Fischer's equation[54] and TEMPO capturing method,[69] respectively. Table 4 summarizes the results. The value of k_a of the EMADC/CuBr system (0.12 M^{-1} s^{-1}) was ca. 20 times lower than that of EBiB/CuBr (2.7 M^{-1} s^{-1}) with the same ligand, PMDETA (entries 1 and 2). However, the value of k_{da} ($= k_a/K_{ATRP}$) was ca. 2 times higher with the EMADC/CuBr system, which provides a reason for well-controlled polymerization with DC initiators. Changing EMADC to MANDC in the presence of PMDETA resulted in a value for k_a which was 10 times higher, explaining why MMA polymerization was successful with the MANDC initiator (entries 1 and 3). The value of k_a in entry 4 indicated that EMADC with HMTETA/CuBr (0.0075 M^{-1} s^{-1}) was ca. 15 times lower than that of the same initiator with PMDETA/CuBr. On the other hand, the k_a for entry 6 indicated that MANDC with HMTETA/CuBr (0.016 M^{-1} s^{-1}) was ca. 70 times lower than that of MANDC with PMDETA/CuBr. The k_a values between Me_6TREN and HMTETA with EMADC/CuBr were almost identical (0.0077 and 0.0075 M^{-1} s^{-1}, respectively). This is in substantial contrast to activation of alkyl bromides, for which a CuBr/Me_6TREN is ∼1000 times more active than CuBr/PMDETA. This indicates that complexes with different ligand activate alkyl (pseudo)halides very selectively. The value of k_a of the EMADC/Me_6TREN system (entry 7) was very low, which explains why, as shown below, polymerization with Me_6TREN resulted in polymers with high PDI. The value of K_{ATRP} of EMADC with PMDETA/CuBr (2.0×10^{-9}) indicated that it was ca. 40 times lower than that of EBiB with PMDETA/CuBr (7.5×10^{-8}) and that of MANDC with PMDETA/CuBr (8.8×10^{-8}). The value of k_{da} of EBiB with PMDETA/CuBr (3.6×10^7 M^{-1} s^{-1}) was 3 times higher than that of MANDC with PMDETA/CuBr (1.3×10^7 M^{-1} s^{-1}) but was 2 times lower than that of EMADC with PMDETA/CuBr (6.1×10^7 M^{-1} s^{-1}). Entry 8 shows that the halogen initiator (EBiB) could be activated by PMDETA/Cu^IDC, as demonstrated above, and that the value of k_a of this system was 7 times larger than that of EMADC with the same complex, but 3 times smaller than the k_a of EBiB with PMDETA/CuBr complex. Generally, the k_{da} values of systems studied in this work were comparable to that of normal ATRP. The activity of the initiators as a function of substituents increased in the order of ester < cyano while the activity of the ligands increased in the order Me_6TREN ≈ HMTETA ≪ PMDETA.

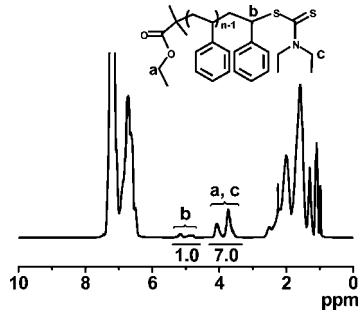

Figure 9. ^1H NMR (in $CDCl_3$) spectroscopy of PSt macroinitiator (M_n = 1900, M_w/M_n = 1.06) prepared with the St/EMADC/CuBr/PMDETA (= 100/1/2/6) in bulk at 120 °C.

End-Group Analyses and Chain Extension. PSt macroinitiator (M_n = 1900, M_w/M_n = 1.06) was dissolved in $CDCl_3$, and analysis of the end-group of the polymer chain was conducted by ^1H NMR (Figure 9). The peaks at 3.6−4.1 ppm are due to the mixture of methylene protons, a and c, of the EMADC initiator. The peaks at 4.8−5.2 ppm correspond to the methine proton, b, adjacent to the terminal DC group. The ratio of the peaks at 3.6−4.1 ppm (a + c) to the peaks at 4.8−5.2 ppm (b) is 7:1, which is quite close to the theoretical value 6:1. This result confirms the existence of the DC group at the polymer chain end.

To confirm the retention of the DC group at the chain end and demonstrate the living character of the polymerization, chain extension from the PSt macroinitiator (M_n = 1900, M_w/M_n = 1.06) was conducted with St. Chain extension was carried out at 120 °C with the ratio of St/macroinitiator/CuBr/PMDETA = 200/1/1/2. After 340 min reaction, a completely chain

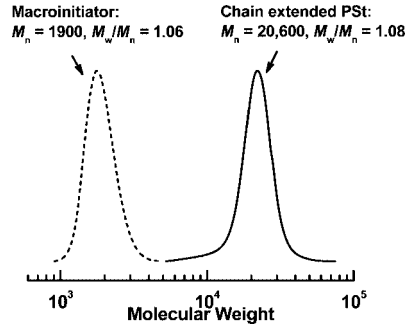

Figure 10. GPC traces of PSt macroinitiator before (dotted line) and after (solid line) chain extension with St. Experimental conditions for chain extension with St: St/PSt macroinitiator/CuBr/PMDETA = 200/1/1/2 in bulk at 120 °C.

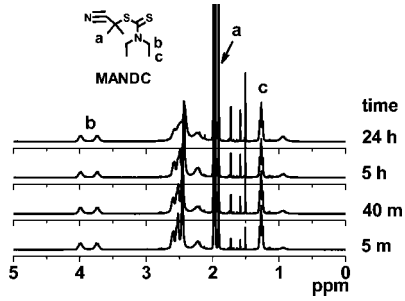

Figure 11. ^{1}H NMR spectra for the mixture of MANDC, CuBr, and PMDETA in acetonitrile-d_3 under a N_2 atmosphere (rt): $[MANDC]_0 = [CuBr]_0 = [PMDETA]_0 = 50$ mM.

extended PSt (M_n = 20 600, M_w/M_n = 1.08) was observed without any unreacted macroinitiator remaining (Figure 10). This demonstrates that the DC group at the PSt chain end allows clean chain extension with St, while retaining low PDI. The above data indicate that the DC group is maintained at the chain end.

(Pseudo)Halogen Exchange. The results of end-group analysis and chain extension are in agreement with the previously reported results.[44−48] However, they were reported for polymers, so an exact quantification could not be made. To further confirm and analyze end-group purity, we followed the chain-end composition by ^{1}H NMR in low-molar-mass model systems. First, MANDC, CuBr, and PMDETA (50 mM) were mixed in MeCN-d_3 in an NMR tube, and the ^{1}H NMR spectra were measured (Figure 11). All the peaks of MANDC, a (1.89−1.91 ppm), b (3.61−4.11 ppm), and c (1.22−1.39 ppm), remained constant. Apparently, no change was observed in NMR spectra over 24 h at rt. The above result indicates that MANDC was activated to produce a MAN radical and a DCCu^{II}Br complex, but this radical was deactivated by the DC group in the deactivator not by the Br. In other words, this experiment demonstrates negligible "halogen exchange" between the DC present in the initiator and the Br in the catalyst.

Next, EBiB, Cu^{I}DC, and PMDETA (50 mM) were mixed, and the reaction was monitored by ^{1}H NMR (Figure 12). The spectrum at time zero was measured in the presence of EBiB and PMDETA. As time went by, the peak at 4.2 ppm (corresponding to a in EBiB) gradually decreased and almost disappeared after 35 min, while the intensity of the peak at 4.1 ppm (corresponding to a′ at EMADC) gradually increased. Because no EMADC was added initially, these observations indicate that EBiB is activated by the Cu^{I}DC complex, and then the DC group in the catalyst replaces Br in EBiB after termination. These results show that the DC group preferentially exists at the growing chain end, irrespective of whether bromide or DC initiator is used with PMDETA ligand. The formed

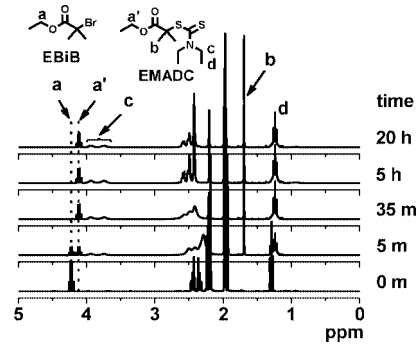

Figure 12. ^{1}H NMR spectra for the mixture of EBiB, Cu^{I}DC, and PMDETA in acetonitrile-d_3 under a N_2 atmosphere (room temperature): $[EBiB]_0 = [Cu^IDC]_0 = [PMDETA]_0 = 50$ mM.

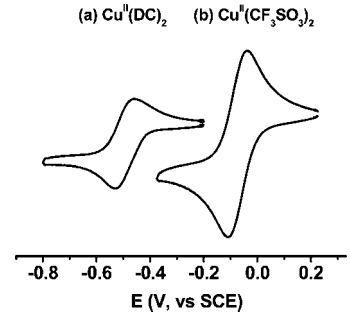

Figure 13. Cyclic voltammogram recorded at 25 °C at a glassy carbon electrode in an acetonitrile solution of (a) Cu^{II}(DC)$_2$/Me$_6$TREN (1.0 mM) and (b) Cu^{II}(CF$_3$SO$_3$)$_2$/Me$_6$TREN (1.0 mM). 0.1 M NBu$_4$PF$_6$, scan rate 0.10 V s^{-1}; potentials reported vs SEC.

carbon radical prefers DC to halogen, and the copper complex favors halogen over DC.

Redox Potential and (Pseudo)halidophilicity. The activity of the ATRP catalyst is directly related to its reducing powder, i.e., the redox potential of the couple Cu^{II}L$_n$/Cu^{I}L$_n$.[70] The redox potential is in turn related to the relative stabilization of the Cu^{II} vs the Cu^I state by the ligand L. For ligands forming 1:1 complexes with copper ions, the following relation holds:[13]

$$E = E^0 + \frac{RT}{F}\left(\ln\frac{[Cu^{II}]_{tot}}{[Cu^I]_{tot}} - \ln\frac{1+\beta^{II}[L]}{1+\beta^{I}[L]}\right) \approx E^0 + \frac{RT}{F}\left(\ln\frac{[Cu^{II}]_{tot}}{[Cu^I]_{tot}} - \ln\frac{\beta^{II}}{\beta^{I}}\right) \quad (1)$$

where β^j is the stability constant of the complex of Cu^j. The β^{II}/β^I in the eq 1 can be translated into $K_{halido\,Cu^{II}}/K_{halido\,Cu^I}$, which can be calculated from the value of redox potential, where K_X is the (pseudo)halidophilicity[13] of the complex of Cu^{II} and Cu^I (eq 2).

$$X^- + Cu^{II}L_n \overset{K_X}{\rightleftharpoons} XCu^{II}L_n \quad (2)$$

One of the interesting results for ATRP with DC-based copper catalysts is that the complex has more reducing power and a DC anion has higher affinity to Cu^{II}/Me$_6$TREN complex than those of halide anions (Br$^-$ and Cl$^-$). Redox potentials of Cu^{II}DC$_2$ and Cu^{II}(CF$_3$SO$_3$)$_2$ were measured at 25 °C with a Gamry Reference 600 potentiostat. Redox potential ($E_{1/2}$, vs SEC) of Cu^{II}DC$_2$ and Cu^{II}(CF$_3$SO$_3$)$_2$ with Me$_6$TREN were −0.495 and −0.07 V, respectively (Figure 13). As can be seen in Table 5, $E_{1/2}$ for Cu^{II}(CF$_3$SO$_3$)$_2$, Cu^{II}Br$_2$, Cu^{II}Cl$_2$, and Cu^{II}DC$_2$ with Me$_6$TREN was −0.07, −0.30, −0.413, and −0.495 V,

Table 5. Cyclic Voltammetry of $Cu^{II}X_2$/Me_6TREN Complexes in MeCN at 25 °C[a]

counterion (X)	$E_{p,a}$/V	$E_{p,c}$/V	$E_{1/2}$/V	$K_{halido\ Cu^{II}}/K_{halido\ Cu^{I}}$	reference
CF_3SO_3	−0.038	−0.109	−0.07		this work
Br	−0.240	−0.355	−0.300	$10^{3.9}$	70
Cl	−0.350	−0.475	−0.413	$10^{5.8}$	70
DC	−0.461	−0.529	−0.495	$10^{7.2}$	this work

[a] 0.1 M NBu_4PF_6, 1.0 mM $Cu^{II}X_2$/Me_6TREN complex, scan rate 0.10 V s^{-1}; potentials reported vs SCE; $E_{p,a}$ and $E_{p,c}$ are the peak potentials of the oxidation and reduction waves, respectively; $E_{1/2} = (E_{p,a} + E_{p,c})/2$.

Scheme 3. Proposed Mechanism of the ATRP with Alkyl Diethyldithiocarbamate/CuBr/ligand System

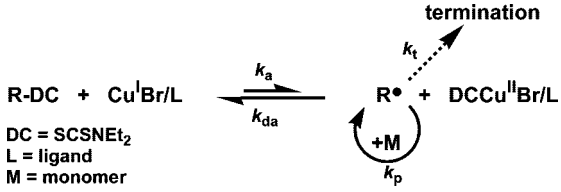

respectively, which indicates the $Cu^{II}DC_2$ is the most reducing and the $Cu^{II}(CF_3SO_3)_2$ is the least reducing among these complexes. The ratio of K_X of Cu^{II} ($K_{halido\ Cu^{II}}$) compared to that of Cu^{I} ($K_{halido\ Cu^{I}}$) using Br, Cl, and DC as a counterion increased from $10^{3.9}$, $10^{5.8}$ to $10^{7.2}$. The relative value of K_X for DC complex was 25 and 2000 times larger than that with Cl and Br complex, respectively. This result encourages us to investigate ATRP in protic media because the value of K_X is substantially lower in protic media than in aprotic solvents so that the deactivators are unstable,[71] resulting in uncontrolled polymerization. This investigation is currently in progress in our group. Typical values of K_X in aprotic solvents are of the order of 10^4-10^5 M^{-1} [72] or higher, whereas in protic solvents these values are 2 or more orders of magnitude lower.[71]

Mechanism of Polymerization. Based on the model study, polymer chain-end analysis by ^1H NMR, and successful chain extension, the proposed polymerization mechanism for this initiation system is shown in Scheme 3, by analogy with transition metal catalyzed atom transfer radical addition. The transition metal catalyst (CuBr/L, L = ligand) reacts with a pseudohalide initiator (R−DC), generating a radical and an oxidized transition metal complex (DCCu^{II}Br/L) by transferring the pseudohalogen (DC) to the catalyst. The radical propagates by reaction with M and is rapidly and preferentially deactivated by DC rather than the halogen in the DCCu^{II}Br/L complex to re-form the original catalyst and an oligomeric pseudo-halide molecule. This process repeats many times, as in a normal ATRP, resulting in a controlled polymerization and formation of a polymer with low PDI.

Conclusions and Future Outlook

Well-controlled polymerizations of both St and MMA with a novel series of DC initiators—ANDC, MANDC, EMADC, and MPADC—and with Cu complexes with nitrogen-based ligands resulted in low polymers with polydispersity (M_w/M_n < 1.1 (St) and M_w/M_n < 1.2 (MMA)). Initiator structure significantly affects the level of control in the polymerization, i.e., the bulkier the substituent adjacent to the sulfur atom in the initiators, the more efficient initiation; also, a cyano substituent in the initiator resulted in a faster initiation than did an ester. The polymerization rate followed first-order kinetics with respect to monomer conversion, and molecular weights increased linearly up to high conversion. It was determined that the polymer chain end is a DC group, indicating negligible exchange between the DC group and halogen in the copper complex and, furthermore, that the polymer chain end is cleanly chain extended to a higher molecular weight polymer. Ligand structure also affects the level of control in a polymerization: PMDETA is one of the best ligands for St polymerization, followed by BPMODA, HMTETA, and TMEDA. For MMA polymerizations, bpy and TMEDA were the best, followed by HMTETA and BPMODA. The values of k_{da} were similar to those for Br-based ATRP, which explains the reason for the well-controlled polymerization, although k_as were smaller than the values in Br-based ATRPs. R_p increased with increased ratio of ligand to metal for the bulk ATRP of St and reached a maximum at ligand:copper ratio of 1:1, but decreased with further increase in the amount of ligand. The $Cu^{II}DC_2$ complex showed higher halidophilicity than that of $Cu^{II}Cl_2$ or $Cu^{II}Br_2$ complex, which should be promising candidates for ATRP in protic media. Furthermore, the DC group can be activated by UV irradiation, resulting in photocontrolled ATRP, which is currently studied in our laboratory.

Acknowledgment. The authors thank the National Science Foundation (CHE-07-15494) and the members of the CRP Consortium at Carnegie Mellon University for their financial support. The authors thank Wade A. Braunecker and Nicolay V. Tsarevsky for the CV measurements and helpful discussions.

References and Notes

(1) Matyjaszewski, K., Davis, T. P., Eds. *Handbook of Radical Polymerization*; Wiley-Interscience: Hoboken, 2002.
(2) Matyjaszewski, K., Gnanou, Y., Leibler, L., Eds. *Macromolecular Engineering. Precise Synthesis, Materials Properties, Applications*; Wiley-VCH: Weinheim, 2007.
(3) Matyjaszewski, K.; Spanswick, J. *Mater. Today* **2005**, *8*, 26–33.
(4) Braunecker, W. A.; Matyjaszewski, K. *Prog. Polym. Sci.* **2007**, *32*, 93–146.
(5) Goto, A.; Fukuda, T. *Prog. Polym. Sci.* **2004**, *29*, 329–385.
(6) Georges, M. K.; Veregin, R. P. N.; Kazmaier, P. M.; Hamer, G. K. *Macromolecules* **1993**, *26*, 2987–2988.
(7) Hawker, C. J.; Bosman, A. W.; Harth, E. *Chem. Rev.* **2001**, *101*, 3661–3688.
(8) Wang, J.-S.; Matyjaszewski, K. *Macromolecules* **1995**, *28*, 7901–7910.
(9) Wang, J.-S.; Matyjaszewski, K. *J. Am. Chem. Soc.* **1995**, *117*, 5614–5615.
(10) Kato, M.; Kamigaito, M.; Sawamoto, M.; Higashimura, T. *Macromolecules* **1995**, *28*, 1721–1723.
(11) Matyjaszewski, K.; Xia, J. *Chem. Rev.* **2001**, *101*, 2921–2990.
(12) Kamigaito, M.; Ando, T.; Sawamoto, M. *Chem. Rev.* **2001**, *101*, 3689–3745.
(13) Tsarevsky, N. V.; Matyjaszewski, K. *Chem. Rev.* **2007**, *107*, 2270–2299.
(14) Chiefari, J.; Chong, Y. K.; Ercole, F.; Krstina, J.; Jeffery, J.; Le, T. P. T.; Mayadunne, R. T. A.; Meijs, G. F.; Moad, C. L.; Moad, G.; Rizzardo, E.; Thang, S. H. *Macromolecules* **1998**, *31*, 5559–5562.
(15) Moad, G.; Rizzardo, E.; Thang, S. H. *Aust. J. Chem.* **2006**, *59*, 669–692.
(16) Moad, G.; Rizzardo, E.; Thang, S. H. *Polymer* **2008**, *49*, 1079–1131.
(17) Yamago, S.; Iida, K.; Yoshida, J. *J. Am. Chem. Soc.* **2002**, *124*, 2874–2875.
(18) Yamago, S.; Ray, B.; Iida, K.; Yoshida, J.; Tada, T.; Yoshizawa, K.; Kwak, Y.; Goto, A.; Fukuda, T. *J. Am. Chem. Soc.* **2004**, *126*, 13908–13909.
(19) Yamago, S.; Kayahara, E.; Kotani, M.; Ray, B.; Kwak, Y.; Goto, A.; Fukuda, T. *Angew. Chem., Int. Ed.* **2007**, *46*, 1304–1306.
(20) Yamago, S. *J. Polym. Sci., Part A: Polym. Chem.* **2005**, *44*, 1–12.
(21) Goto, A.; Zushi, H.; Hirai, N.; Wakada, T.; Tsujii, Y.; Fukuda, T. *J. Am. Chem. Soc.* **2007**, *129*, 13347–13354.
(22) Singha, N. K.; Klumperman, B. *Macromol. Rapid Commun.* **2000**, *21*, 1116–1120.
(23) Davis, K. A.; Matyjaszewski, K. *J. Macromol. Sci., Pure Appl. Chem.* **2004**, *41*, 449–465.
(24) Braunecker, W. A.; Itami, Y.; Matyjaszewski, K. *Macromolecules* **2005**, *38*, 9402–9404.
(25) Brandts, J. A. M.; van de Geijn, P.; van Faassen, E. E.; Boersma, J.; Van Koten, G. *J. Organomet. Chem.* **1999**, *584*, 246–253.
(26) Maria, S.; Stoffelbach, F.; Mata, J.; Daran, J.-C.; Richard, P.; Poli, R. *J. Am. Chem. Soc.* **2005**, *127*, 5946–5956.
(27) Matyjaszewski, K.; Wei, M.; Xia, J.; McDermott, N. E. *Macromol-*

ecules **1997**, *30*, 8161–8164.
(28) Ando, T.; Kamigaito, M.; Sawamoto, M. *Macromolecules* **1997**, *30*, 4507–4510.
(29) Matyjaszewski, K.; Jakubowski, W.; Min, K.; Tang, W.; Huang, J.; Braunecker, W. A.; Tsarevsky, N. V. *Proc. Natl. Acad. Sci. U.S.A.* **2006**, *103*, 15309–15314.
(30) Jakubowski, W.; Matyjaszewski, K. *Angew. Chem., Int. Ed.* **2006**, *45*, 4482–4486.
(31) Jakubowski, W.; Min, K.; Matyjaszewski, K. *Macromolecules* **2006**, *39*, 39–45.
(32) Min, K.; Gao, H.; Matyjaszewski, K. *Macromolecules* **2007**, *40*, 1789–1791.
(33) Dong, H.; Tang, W.; Matyjaszewski, K. *Macromolecules* **2007**, *40*, 2974–2977.
(34) Gillies, M. B.; Matyjaszewski, K.; Norrby, P.-O.; Pintauer, T.; Poli, R.; Richard, P. *Macromolecules* **2003**, *36*, 8551–8559.
(35) Matyjaszewski, K.; Poli, R. *Macromolecules* **2005**, *38*, 8093–8100.
(36) Tang, W.; Matyjaszewski, K. *Macromolecules* **2007**, *40*, 1858–1863.
(37) Otsu, T.; Yoshida, M.; Tazaki, T. *Makromol. Chem., Rapid Commun.* **1982**, *3*, 133–140.
(38) Otsu, T.; Matsumoto, A. *Adv. Polym. Sci.* **1998**, *136*, 75–137.
(39) Otsu, T. *J. Polym. Sci., Part A: Polym. Chem.* **2000**, *38*, 2121–2136.
(40) Kroeze, E.; de Boer, B.; ten Brinke, G.; Hadziioannou, G. *Macromolecules* **1996**, *29*, 8599–8605.
(41) Higashi, J.; Nakayama, Y.; Marchant, E. R.; Matsuda, T. *Langmuir* **1999**, *15*, 2080–2088.
(42) Ishizu, K.; Katsuhara, H.; Itoya, K. *J. Polym. Sci., Part A: Polym. Chem.* **2006**, *44*, 3321–3327.
(43) Ishizu, K.; Mori, A. *Macromol. Rapid Commun.* **2000**, *21*, 665–668.
(44) Li, P.; Qiu, K.-Y. *J. Polym. Sci., Part A: Polym. Chem.* **2002**, *40*, 2093–2097.
(45) Li, P.; Qin, S.-H.; Qin, D.-Q.; Qiu, K.-Y. *Polym. Int.* **2004**, *53*, 756–765.
(46) Zhang, W.; Zhu, X.; Zhu, J.; Chen, J. *J. Polym. Sci., Part A: Polym. Chem.* **2005**, *44*, 32–41.
(47) Zhang, W.; Zhou, N.; Zhu, J.; Sun, B.; Zhu, X. *J. Polym. Sci., Part A: Polym. Chem.* **2005**, *44*, 510–518.
(48) Zhang, W.; Zhu, X.; Cheng, Z.; Zhu, J. *J. Appl. Polym. Sci.* **2007**, *106*, 230–237.
(49) Zhang, W.; Wang, C.; Li, D.; Song, Q.; Cheng, Z.; Zhu, X. *Macromol. Symp.* **2008**, *261*, 23–31.
(50) Otsu, T.; Matsunaga, T.; Doi, T.; Matsumoto, A. *Eur. Polym. J.* **1995**, *31*, 67–78.
(51) Ishizu, K.; Katsuhara, H.; Kawauchi, S.; Furo, M. *J. Appl. Polym. Sci.* **2005**, *95*, 413–418.
(52) Tang, W.; Matyjaszewski, K. *Macromolecules* **2006**, *39*, 4953–4959.
(53) Akerstrom, S. *Ark. Kemi* **1959**, *14*, 387–401.
(54) Tang, W.; Tsarevsky, N. V.; Matyjaszewski, K. *J. Am. Chem. Soc.* **2006**, *128*, 1598–1604.
(55) The experimental procedure used to determine the values of extinction coefficient (ε) by UV is similar to that provided in the k_a experiment. To measure ε, CuBr/PMDETA (10.0 mM), TEMPO (10.0 mM), and MeCN were mixed in a Schlenk flask joined to a quartz UV cuvette, and degassed EMADC (1.0 mM) was injected via a N_2-purged syringe. After stirring 48 h at rt in a dark place, the flask was transferred to a Cary 5000 UV/vis/NIR spectrometer. The absorbance at a wavelength corresponding to the λ_{max} of the generated Cu^{II} deactivator complex was monitored. $\varepsilon = 750.3$ ($\lambda_{max} = 795$ nm).
(56) Charmot, D.; Corpart, P.; Adam, H.; Zard, S. Z.; Biadatti, T.; Bouhadir, G. *Macromol. Symp.* **2000**, *150*, 23–32.
(57) (a) Matyjaszewski, K.; Jo, S. M.; Paik, H.-j.; Shipp, D. A. *Macromolecules* **1999**, *32*, 6431–6438. (b) Matyjaszewski, K.; Gaynor, S. G.; Coca, S. U.S. Patent 6,541,580, **2003**.
(58) Wang, J.-L.; Grimaud, T.; Shipp, D. A.; Matyjaszewski, K. *Macromolecules* **1998**, *31*, 1527–1534.
(59) Matyjaszewski, K.; Wei, M.; Xia, J.; Gaynor, S. G. *Macromol. Chem. Phys.* **1998**, *199*, 2289–2292.
(60) Xia, J.; Matyjaszewski, K. *Macromolecules* **1997**, *30*, 7697–7700.
(61) Xia, J.; Gaynor, S. G.; Matyjaszewski, K. *Macromolecules* **1998**, *31*, 5958–5959.
(62) Matyjaszewski, K.; Patten, T. E.; Xia, J. *J. Am. Chem. Soc.* **1997**, *119*, 674–680.
(63) Wang, J.-L.; Grimaud, T.; Matyjaszewski, K. *Macromolecules* **1997**, *30*, 6507–6512.
(64) Nanda, A. K.; Matyjaszewski, K. *Macromolecules* **2003**, *36*, 599–604.
(65) Nanda, A. K.; Matyjaszewski, K. *Macromolecules* **2003**, *36*, 1487–1493.
(66) Tang, W.; Nanda, A. K.; Matyjaszewski, K. *Macromol. Chem. Phys.* **2005**, *206*, 1171–1177.
(67) Huang, J.; Pintauer, T.; Matyjaszewski, K. *J. Polym. Sci., Part A: Polym. Chem.* **2004**, *42*, 3285–3292.
(68) Bednarek, M.; Biedron, T.; Kubisa, P. *Macromol. Chem. Phys.* **2000**, *201*, 58–66.
(69) Matyjaszewski, K.; Paik, H.-j.; Zhou, P.; Diamanti, S. J. *Macromolecules* **2001**, *34*, 5125–5131.
(70) Qiu, J.; Matyjaszewski, K.; Thouin, L.; Amatore, C. *Macromol. Chem. Phys.* **2000**, *201*, 1625–1631.
(71) Tsarevsky, N. V.; Pintauer, T.; Matyjaszewski, K. *Macromolecules* **2004**, *37*, 9768.
(72) Ishiguro, S.; Nagy, L.; Ohtaki, H. *Bull. Chem. Soc. Jpn.* **1987**, *60*, 2053.

MA801231R